

See discussions, stats, and author profiles for this publication at: <https://www.researchgate.net/publication/3165903>

DC Flashover of a Dielectric Surface in Atmospheric Conditions

Article in IEEE Transactions on Plasma Science · November 2004

DOI: 10.1109/TPS.2004.835483 · Source: IEEE Xplore

CITATIONS

24

READS

1,226

4 authors, including:



Andreas A Neuber

Texas Tech University

453 PUBLICATIONS 3,157 CITATIONS

[SEE PROFILE](#)



James C Dickens

Texas Tech University

457 PUBLICATIONS 2,940 CITATIONS

[SEE PROFILE](#)

Some of the authors of this publication are also working on these related projects:



Multichannel Signal Synthesis [View project](#)



Design Optimization of MFCG [View project](#)

DC Flashover of a Dielectric Surface in Atmospheric Conditions

John T. Krile, *Member, IEEE*, Andreas A. Neuber, *Senior Member, IEEE*, James C. Dickens, *Senior Member, IEEE*, and Hermann G. Krompholz, *Senior Member, IEEE*

Abstract—Surface flashover is a major consideration in a wide variety of high-voltage applications, and yet has not been studied in great detail for atmospheric conditions, with modern diagnostic tools. Environmental conditions to be considered include pressure, humidity, and gas present in the volume surrounding the dielectric. In order to gain knowledge into the underlying process involved in dielectric surface flashover, a setup has been created to produce and closely monitor the flashover event. Within the setup parameters such as geometry, material, and temporal characteristics of the applied voltage can be altered. Current, voltage, luminosity, and optical emission spectra are measured with nanosecond to subnanosecond resolution. Spatially and temporally resolved light emission data is also gathered along the arc channel.

Our fast imaging data show a distinct trend for the spark in air to closely follow the surface even if an electrical field with a strong normal component is present. This tendency is lacking in the presence of gases such as nitrogen, where the spark follows more closely the electric field lines and develops away from the surface. Further, the breakdown voltage in all measured gases decreases with increasing humidity, in some cases as much as 50% with an increase from 10% relative humidity to 90% relative humidity.

Index Terms—Atmospheric, breakdown, dielectric surface, surface flashover.

I. INTRODUCTION

FOR PARALLEL-PLATE geometries and for certain nonuniform geometries (rod-plane, sphere-sphere, etc.) the volume breakdown process is well known [1]. However, processes involving the presence of a surface (such as secondary electron emission and emission of photoelectrons) have not been investigated with the necessary resolution in the past [2], [3]. Some work has been done on surface discharge along a dielectric surface [4], however the study was more involved with electromagnetic radiation phenomenon associated with lighting than breakdown between two electrodes along an insulator.

Most of the literature data are empirical in nature and there has been disagreement as to whether or not the presence of the surface decreases the breakdown voltage in an atmospheric environment. For example, some sources show the breakdown

voltage being lowered by the presence of a dielectric in the gap [5], [6], while other sources explain the drop in voltage as a result of humidity on the surface, not the surface itself [7].

The only reasonable way to describe surface flashover is a direct simulation of the discharge, considering all the elementary processes contributing to the breakdown event. It has been, however, far from clear which processes are involved to what degree, and what the quantitative parameters and their materials dependence for these processes are.

A practical way to determine the role of elementary processes in the development of surface discharges is a direct measurement of the combined action of these processes as they occur during flashover with high temporal and spatial resolution. Variation of the experimental conditions, for example, to measure streamer development times with and without the surface gives indirect information on surface processes. Along with spectroscopic data, these surface processes could be further narrowed down to, e.g., the role of UV-induced electron emission.

II. EXPERIMENTAL SETUP

It is well known that documenting the dynamics of surface flashover requires a temporal resolution in the nanosecond time regime. Hence, the test apparatus has to be carefully designed to ensure that the shape of the transient signals are due to the flashover itself and not distorted by the external electrical circuit. This high temporal resolution was achieved by designing a surface flashover chamber that exhibits coaxial geometry with 52- Ω impedance, which matches the two coaxial charging lines. The entire setup is shown in Fig. 1 from high-voltage power supply through the charging line, test chamber, reverse polarity charging line, and second power supply.

The traveling wave current sensors, located on the charging lines just outside of the test chamber, have a sensitivity of 0.1 or 0.2 V/A, respectively. To achieve a wider range of resolution, the signal of one of the sensors was amplified by 20 dB before being fed into the high-speed oscilloscope, another was attenuated by 20 dB, and a third was fed straight into the oscilloscope. This enabled us to measure currents in the range from a few milliamperes to 100 A with nanosecond temporal resolution.

The chamber, which we constructed of half-inch-thick clear Lexan, was designed to be filled with any desired gas at atmospheric pressure through a fill port and release valve. The humidity of the gas within the chamber could also be controlled via an ultrasonic humidifier placed prior to the fill line.

About 25 mm away from the electrode gap, a set of three cylindrical rod lenses were used to focus the light emission from the vicinity of anode, cathode, and the center of the insulator

Manuscript received December 11, 2003; revised March 10, 2004. This work was supported by Sandia National Laboratories.

J. T. Krile is with the Center for Pulsed Power and Power Electronics in the Electrical Engineering Department at Texas Tech University, Lubbock, TX 79409 USA (e-mail: JKrile@p3e.ttu.edu).

A. A. Neuber, J. C. Dickens, and H. G. Krompholz are with the Electrical Engineering Department at Texas Tech University, Lubbock, TX 79409 USA (e-mail: A.Neuber@coe.ttu.edu; JDickens@coe.ttu.edu; HermannK@coe.ttu.edu).

Digital Object Identifier 10.1109/TPS.2004.835483

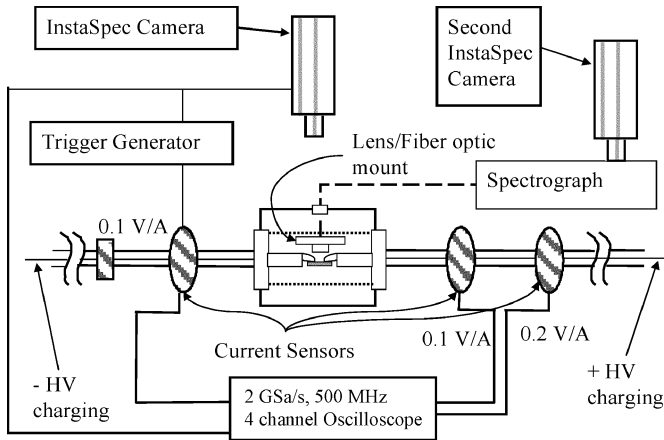


Fig. 1. Experimental setup. The box in the center represents the chamber itself, with the dotted lines showing the wire mesh outer conductor and the dashed line representing the fiber optic cables. Gas filling lines and the 150-kV power supplies are omitted.

into three separate fiber optic cables. These fiber optic cables exit the coaxial chamber through a small hole in the outer conductor and connect to the diagnostics through the feedthroughs in the chamber wall. The output end of the fiber optics was either fed into a spectrograph or into three photomultiplier tubes (PMTs) (Hamamatsu Photonics). The PMTs have a sensitivity in the range of 200 $\mu\text{A}/\text{lm}$ and a fast rise time of 0.78 ns.

We also utilized two fast, intensified CCD cameras (Andor Technologies). One camera was positioned just outside the chamber with a zoom lens attached to capture the pre- and main breakdown paths. This camera was focused on the surface through a small hole in the outer conductor. The second ICCD camera was connected to the output end of a quarter meter imaging spectrograph. Both ICCD cameras were triggered using a TTL gate pulse generated by a trigger-delay generator, which is triggered on the output of one of the current sensors. The trigger gate is also sent to the oscilloscope to synchronize the waveforms with the images. When capturing extremely small pre-breakdowns an amplifier was placed between the current sensor and the trigger generator. While capturing main breakdown an attenuator was used in place of the amplifier. Most experiments were performed with an 80-ns trigger gate, which results in a 68-ns optical gate for the cameras. The majority of tests involving the PMTs or spectrograph were done with the type A electrode geometry, shown in Fig. 1, which exhibits only a weak electric field component normal to the dielectric surface. However, type A electrodes produce a predictable arc path, which is ideal for the optical testing. A second electrode design, type B, was also developed which has a strong electric field component normal to the surface, mainly for additional imaging tests. A final electrode design, type C, was also created to test cylindrical-shaped alumina samples. All three electrode designs are shown in Fig. 2.

III. RESULTS AND DISCUSSION

A. Reference Current Waveforms

All optical emission data (imaging, spectroscopy, PMT) were recorded along with corresponding current waveforms with the

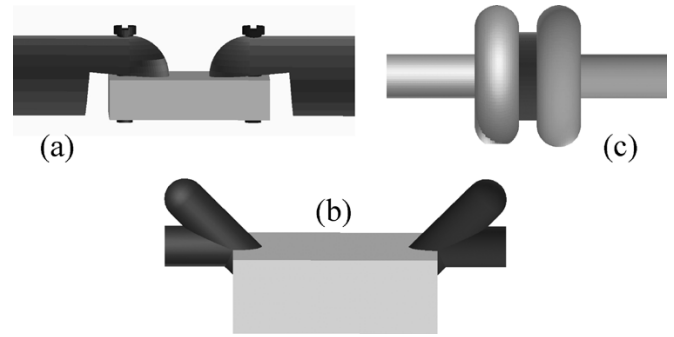


Fig. 2. Various electrode-surface geometries. Geometry B penetrates ~ 10 mm into the surface. All other electrodes are pressed onto the surface.

same or better temporal resolution. In Figs. 3 and 4 are shown a representative set of waveforms with the different regions marked. It should be noted that the negative reflections seen after the initial peak are artifacts of reflections in the charging line and should be disregarded. Also, the waveforms are only intended to provide a general representation of breakdown waveforms. The actual waveforms vary slightly in magnitude and rise/fall time for different test conditions. In the following discussion, we will make references as to when during the breakdown event a particular set of data was acquired.

B. Angled Electrodes, Geometry B, With a Planar Surface

These tests were conducted to ascertain whether the flashover would follow the electric field line, away from the surface, or if it would follow the surface itself. As can be seen in Figs. 5 and 6, the flashover follows to some extent the electric field line in nitrogen but clearly follows the surface in air. The results in argon are not shown, but are very similar to nitrogen.

In air, the pre-breakdown events were documented occurring anywhere from several microseconds up to 100 μs or more before main breakdown to immediately preceding the main breakdown. It was shown that early pre-breakdown in air also follows the surface just as the main breakdown does. The pre-breakdown occurs just as often early as it does right before the main breakdown. Similarly, it was shown that pre-breakdown in nitrogen followed the electric field lines just like a main breakdown in nitrogen.

C. Angled Electrodes, Geometry B, With a Grooved Surface

In order to determine if the flashover would continue to follow the surface in air even if the path distance was greater than or equal to the distance between the electrodes a groove was cut into the surface between the electrodes. In Figs. 7–9, the groove extends perpendicular to the plane of the page.

As can be seen in Figs. 7 and 8, the flashover continues to follow the surface in air, and continues to follow the electric field in nitrogen and argon. Again, these results hold true for pre-breakdown as well; this is shown for an air environment in Fig. 9.

D. Temporally and Spatially Resolved Light Emission

For the PMT tests, the type A electrode geometry is used. In all tests, the first light emission was detected from the cathode. The initial emission, as in Fig. 10, was sometimes in the form

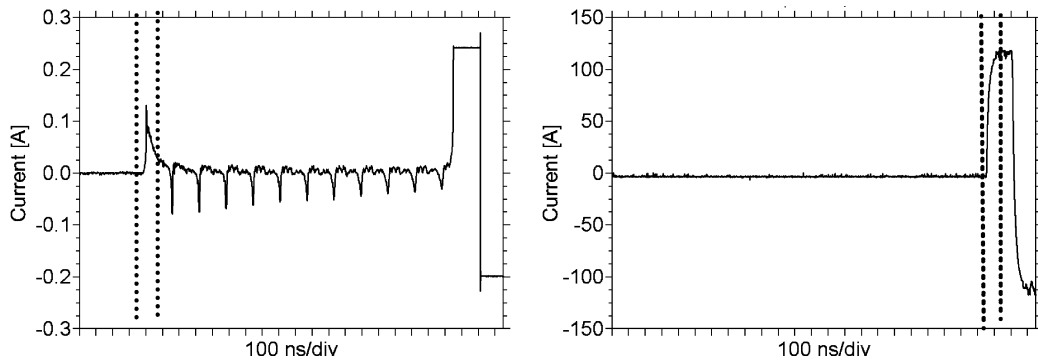


Fig. 3. Current waveform of an early pre-breakdown in air with a 12 mm Lexan gap ($V_b = 20$ kV). The left waveform shows the high sensitivity current, the right waveform represents the current with an impedance limited amplitude of about 120 A. The dotted lines represent the camera gate for early pre-breakdown (left) and main breakdown (right).

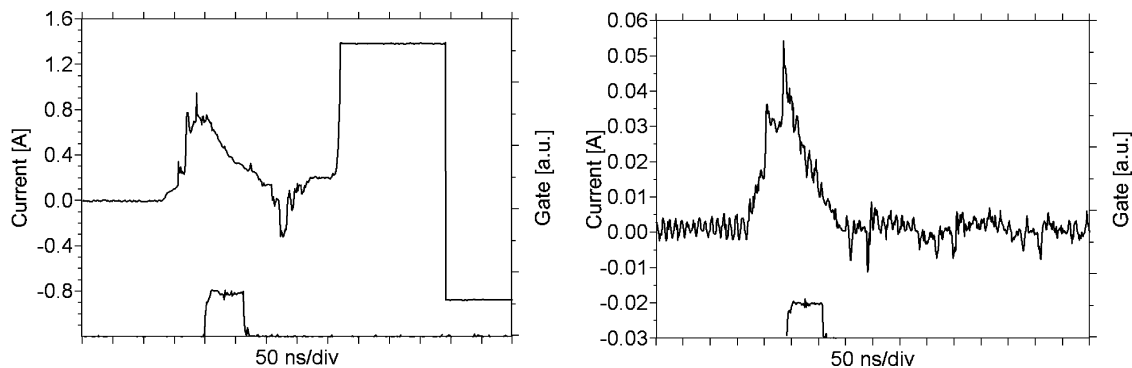


Fig. 4. Amplified current of pre-breakdown just prior to main breakdown in air with a 12 mm Lexan gap ($V_b = 21$ kV). Main breakdown is denoted by the clipped signal, and a very early pre-breakdown is shown on the right. The lower waveform represents the camera 80 ns exposure gate.

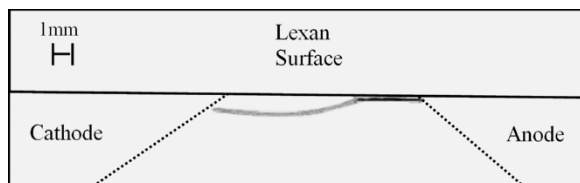


Fig. 5. Side-on photo negative image of main breakdown in nitrogen with planar surface, 11-mm gap. Breakdown voltage $V_b = 11$ kV.

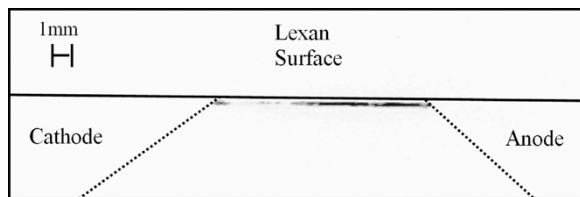


Fig. 6. Side-on photo negative image of main breakdown in air with planar surface, 11-mm gap. Breakdown voltage $V_b = 20$ kV.

of an early spike. The early spike represents the initial electron emission from the cathode, which successively causes electron impact excitation of the gas. This spike is different from a normal pre-breakdown, which can also be seen in Fig. 10 as occurring approximately 150 ns after the initial spike seen at the cathode. The pre-breakdown occurs approximately $1.7 \mu\text{s}$ prior to the main breakdown, which is denoted by the clipped signal.

Using three PMTs and focusing on the main breakdown, as in Fig. 11, it can be seen that the flashover is again initiated at the

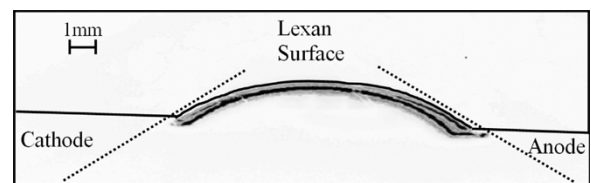


Fig. 7. Side-on photo negative image of main breakdown in air with groove, 12-mm Lexan gap. Breakdown voltage $V_b = 25$ kV.

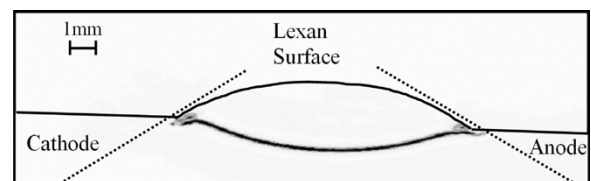


Fig. 8. Side-on photo negative image of main breakdown in nitrogen with groove, 12-mm Lexan gap. Breakdown voltage $V_b = 23.8$ kV.

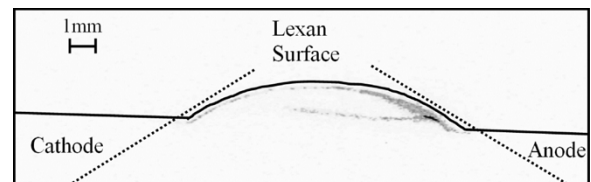


Fig. 9. Side-on photo negative image of pre-breakdown in air with groove, 12-mm Lexan gap. Pre-breakdown voltage $V_{pb} = 37.5$ kV.

cathode. That is, cathode signal indicates light emission occurring at the cathode first, followed by continuous emission from

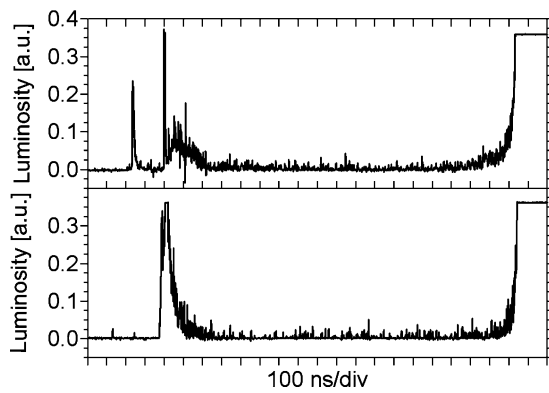


Fig. 10. Measured luminosity from a planar surface in air with an early pre-breakdown and a main breakdown captured. The top is from the cathode fiber and the bottom is from the anode fiber. The PMT signal is clipped during main breakdown in the right half of the figure.

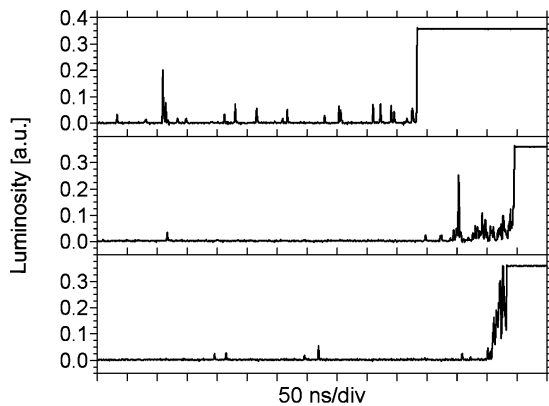


Fig. 11. Measured luminosity across a planar surface in air. Main breakdown $V_b = 20$ kV. The top curve is from the cathode optical fiber, the middle from the center of the Lexan, and bottom is from the anode.

the cathode for the remainder of the breakdown. The electron avalanche traveled across the gap and was amplified, causing the anode signal to grow considerably before the light emission from the gap center exhibits a steep increase due to the cathode directed streamer finally bridging the gap. The cathode emissions are followed by light emission from the anode about 100 to 150 ns later, thus indicating an electron avalanche moving from cathode to anode with about 0.1 mm/ns. The calculated electron drift velocity using equivalent field strength is 0.08 mm/ns, which is on the order of the avalanche velocity [8].

E. Flashover Optical Emission Spectroscopy

The next figures show the spectra measured at just in front of each electrode and the center of the gap. The spectra were collected using a grating with a 150-lines/mm and 300-nm blaze angle, with data being collected from 150 to 800 nm. The lines identified originate from copper and zinc, which stem from the brass electrodes. The presence of magnesium is also possible, however, because only singular a line is detected, it could be a false match. These lines are identified in Fig. 12. Also, the hydrogen line and increased UV content is detected in the spectra gathered in air. Unfortunately, to gain a wider spectral window some resolution is sacrificed. As a result of this tradeoff, further line identification is difficult; however, the presence of the

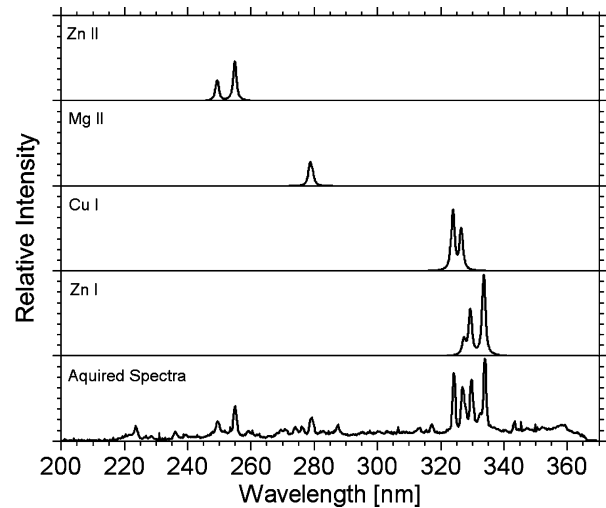


Fig. 12. Simulated spectra for various elements is used to identify major peaks in the acquired spectra.

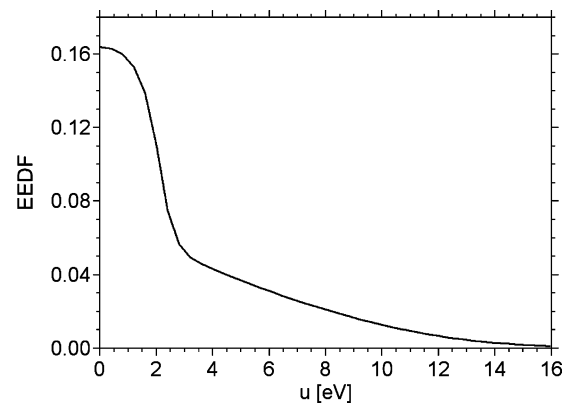


Fig. 13. Electron energy distribution function at breakdown in a pure nitrogen environment.

hydrogen line and the increased UV content in air provides valuable information on the process of surface flashover.

Following the presented experimental data, we draw the following picture of surface flashover at atmospheric pressure. The presence of the dielectric surface in nitrogen has (besides causing field enhancement at the dielectric–gas–metal triple point) little influence on the discharge development in the gap, specifically for geometries with a nonnegligible normal field component. In detail, the average electron energy at the flashover threshold is estimated to be about 4.5 eV, which would correspond to a wavelength of about 280 nm for radiation caused by electrons with this energy. However, the electron energy distribution function exhibits significant contributions up to ~ 15 eV as shown in Fig. 13. These values and the EEDF are obtained using a program that calculates the electron energy distribution function for various conditions [8]. The E/N value was adjusted so that the effective ionization frequency (ionization—attachment, recombination) approached zero or slightly positive values consistent with volume breakdown conditions.

Obviously, this energy is still below the first cross-over point for secondary electron emission, SEE, due to impacting electrons (typically on the order of 30 eV for dielectrics) so that the electrons that impact the surface will be trapped in the bulk of

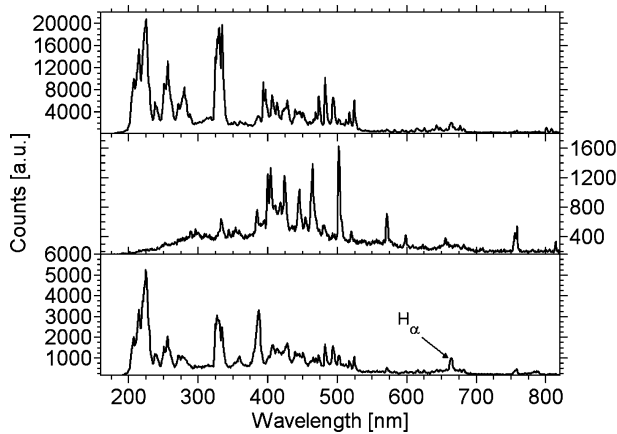


Fig. 14. Full breakdown event (100 μ s gate) in nitrogen. The anode spectrum is on top, the cathode is on bottom and the middle is the middle of the Lexan.

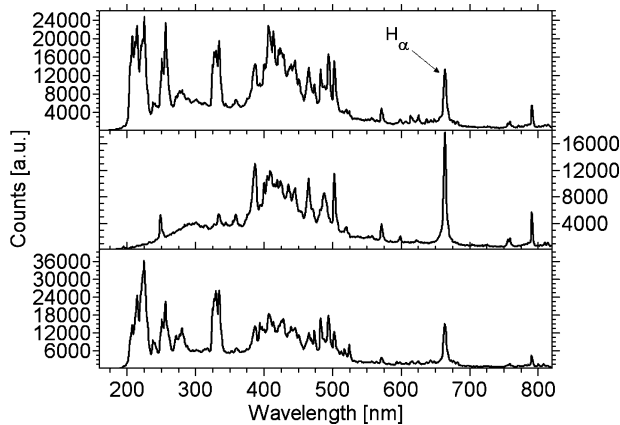


Fig. 15. Full breakdown event (100 μ s gate) in air. The anode spectrum is on top, the cathode is on bottom and the middle is the middle of the Lexan.

the dielectric [3]. Hence, the surface will be negatively charged and the head of any electron avalanche that is developing across the gap will be repelled from the surface, which we believe is true for N_2 or Ar.

As experimentally observed, the situation is different for air with its oxygen component. Here, we use a positive surface charge due to photoemission to explain the arc-channel development close to the surface. An arc in air (oxygen) is known to produce more UV than an arc in pure nitrogen. Quantum yields for photoemission from materials such as Teflon or Polyethylene increase distinctly for photon energies above 5–7 eV ($\gamma_\nu > 10^{-4}$). Hence, we believe that the higher UV content of the excited air is responsible for releasing electrons from the surface causing a net positive charge that attracts the electron avalanche head causing the discharge to develop close to the surface. Unfortunately, our spectroscopy down to 200 nm (~ 6.2 eV) delivers only inconclusive results about a higher UV content in oxygen; cf. Figs. 14 and 15. A closer look at the spectra with higher resolution at the UV-to-deep-UV wavelengths would be necessary. It should also be valuable in the future to extend the spectroscopic results into the VUV region, for instance by reducing the absorption distance from the arc channel to the spectrograph.

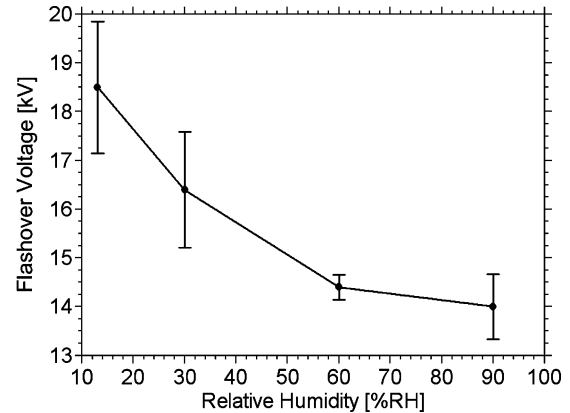


Fig. 16. Breakdown voltage of a Lexan surface in air with varying relative humidity, error bars represent standard deviation of samples at each point. Electrode geometry A is used with a gap spacing of 12 mm.

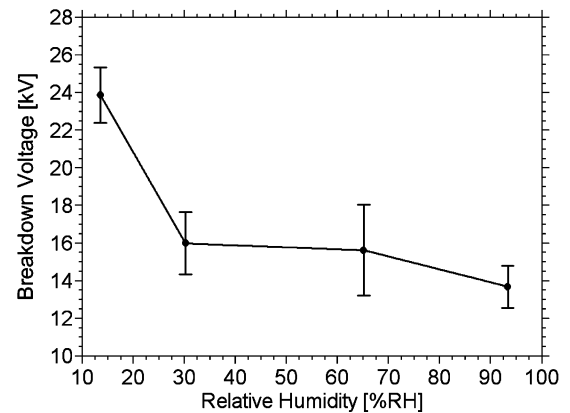


Fig. 17. Breakdown voltage of a Lexan surface in nitrogen with varying relative humidity, error bars represent standard deviation of samples at each point. Electrode geometry A is used with a gap spacing of 12 mm.

The fact that oxygen as a strongly electronegative gas scavenges electrons does additionally favor the flashover development in air close to the surface if, as outlined above, the surface is considered as a source of electrons due to photoemission. The question is which mechanism, repulsion/attraction of the electron avalanche by surface charges or simply photoemission from the surface as additional electron source in air, is dominant, but cannot be conclusively answered and deserves our future attention.

F. Effects of Humidity

In order to determine the effects of humidity on the breakdown voltage, an ultrasonic humidifier was placed inline with the supply of compressed gas. The humidity was then set to four different values, and the breakdown voltages recorded for each level. The results can be seen in Fig. 16 for air and Fig. 17 for nitrogen across a flat Lexan surface. These results confirm the previous finding regarding relative humidity and breakdown voltage [7], [9]. In addition tests were performed using electrode types C and an alumina surface. The alumina results for air and nitrogen environment are shown in Fig. 18 and 19. It is believed that the humidity affects the breakdown voltage by creating a thin layer of water on the surface (adsorption), which is more easily ionized. The higher the humidity the thicker the layer on

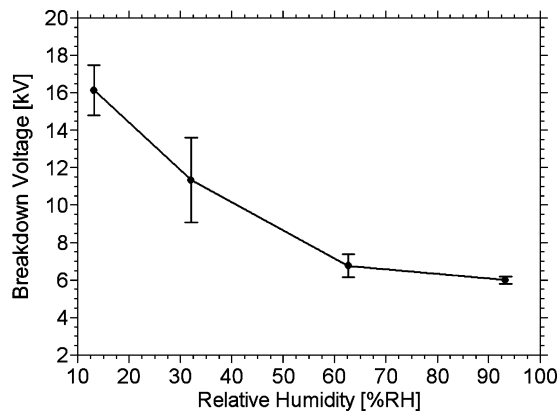


Fig. 18. Breakdown voltage in nitrogen versus relative humidity with an alumina surface. Electrode geometry A is used with a gap spacing of 12 mm.

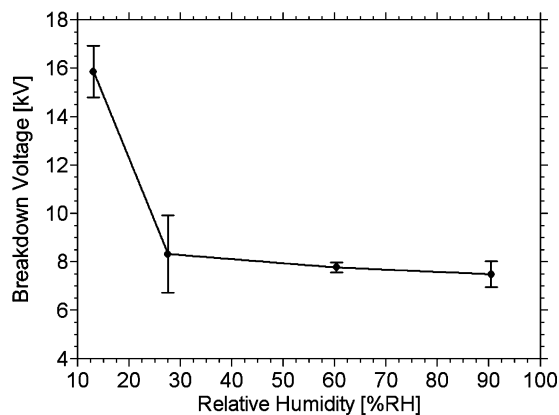


Fig. 19. Breakdown voltage in air versus relative humidity with an alumina surface. Electrode geometry A is used with a gap spacing of 12 mm.

the surface, the easier it is for the field-emitted electrons to produce secondary electrons.

IV. EFFECT OF DIELECTRIC ON BREAKDOWN VOLTAGE

The variation of the breakdown strength with and without the presence of a dielectric surface provides an additional detail to this investigation. To this end, multiple tests were performed with and without the surface present in air and in nitrogen. The baseline results for these tests can be seen in Figs. 20 and 21.

It is experimentally observed that in an air environment the presence of the surface lowered the breakdown voltage by approximately 10%. However, in nitrogen the presence of the surface increased the breakdown voltage by approximately 15%. We speculate that the reason for this lies in surface charge or photoemission from the surface in oxygen. As stated above, in nitrogen environments the electrons lack the energy necessary to liberate secondary electrons from the surface, and are instead trapped by the surface. It was also stated that the surface has little effect on the breakdown aside from the field enhancements at the triple point. It is believed that this field enhancement is actually detrimental to the field strength. The net negative charge of the surface weakens the field at the cathode. This in turn reduces field electron emission, reducing the number of electron to

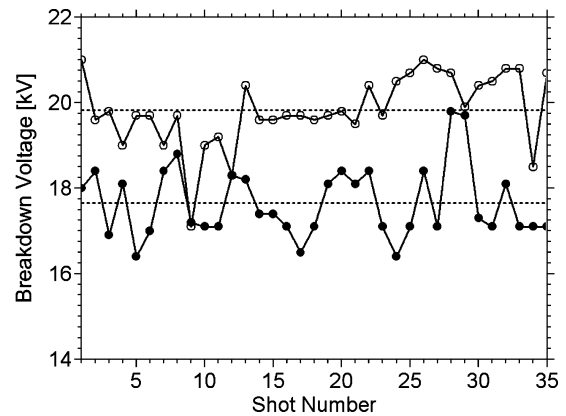


Fig. 20. Breakdown voltage and averages in air both with (bottom curve, closed circles) and without (top curve, open circles) the Lexan surface present. Electrode geometry A is used with a gap spacing of 12 mm.

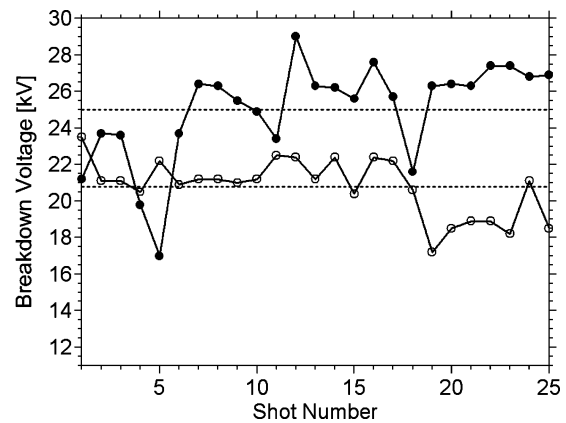


Fig. 21. Breakdown voltage and averages in nitrogen both with (top curve, closed circles) and without (bottom curve, open circles) the Lexan surface present. Electrode geometry A is used with a gap spacing of 12 mm.

be multiplied, and thus decreases the likelihood of breakdown. A higher voltage is necessary in order to produce a sufficient amount of field-emitted electrons from the cathode.

V. CONCLUSION

Profound differences have been documented in the flashover behavior across a dielectric surface between air and nitrogen environments. These differences include arc channel development path and breakdown voltage dependence on the presence of the surface. We believe that these differences are caused by two possible mechanisms. First, there is photoemission in air, which liberates photoelectrons from the surface generating a net positive charge. The second mechanism is the electronegative oxygen in air scavenging electrons released from the surface further increasing the positive space charge of the surface. This positive surface charge causes the flashover to stay near the surface. In a nitrogen environment, the other possible mechanism is the absorption of electrons by the surface due to the lack of sufficient energy for secondary electron emission. The adsorbed electrons produce a net negative surface charge, which repels the head of any electron avalanches. This causes the flashover in nitrogen to follow the electric field lines as opposed to the surface.

ACKNOWLEDGMENT

The authors would like to thank R. E. Jorgenson and L. K. Warne in the Electromagnetics and Plasma Physics Analysis Department for their support.

REFERENCES

- [1] J. M. Meek and J. D. Craggs, *Electrical Breakdown of Gases*. New York: Wiley, 1978.
- [2] H. Miller, "Surface flashover of insulators," *IEEE Trans. Electr. Insul.*, vol. 24, pp. 765–786, Oct. 1989.
- [3] R. E. Jorgenson and L. K. Warne, "Effect of dielectric photoemission on surface breakdown: An LDRD report," Sandia National Laboratories, Albuquerque, NM, Report SAND2000-3044, June 2003.
- [4] A. Bondiou, G. Labaune, and J. P. Marque, "Electromagnetic radiation associated with the formation of an electric breakdown in air at atmospheric pressure," *J. Appl. Phys.*, vol. 61, no. 2, pp. 503–509, Jan. 15, 1987.
- [5] E. Nasser, *Fundamentals of Gaseous Electronics*. New York: Wiley-Interscience, 1971.
- [6] Y. Raizer, *Gas Discharge Physics*. New York: Springer-Verlag, 1991.
- [7] E. Hippauf, "Influence of water on the flashover strength of insulators," *Z. Phys.*, vol. 82, p. 803, 1933.
- [8] A. P. Napartovich, "EEDF: Program for the computation of the electron energy distribution function," State Science Center of Russian Federation Troitsk Institute for Innovation and Fusion Research, Troitsk, Moscow region, Russia, 1993.
- [9] F. W. Maxstadt, "Insulator arcover in air," *Electr. Eng.*, vol. 53, pp. 1062–1068, July 1934.



John T. Krile (M'98) was born in Terra Haute, IN, on June, 2, 1979. He received the M.S. degree in electrical engineering from Texas Tech University, Lubbock, in 2003, and is currently pursuing the Ph.D. degree in electrical engineering at Texas Tech University.

He is working as a Research Assistant at the Center for Pulsed Power and Power Electronics at Texas Tech University while completing his doctoral work.



Andreas A. Neuber (M'97–SM'03) was born in Aschaffenburg, Germany. He received the Dipl.-Phys. and Ph.D., ME, degrees from the Darmstadt University of Technology, Darmstadt, Germany, in 1990 and 1996, respectively.

He was a full-time scientific employee at the Institute of Energy and Power Plant Technology, Darmstadt University of Technology, from 1990 to 1996, in the area of nonlinear laser spectroscopy and chemical reaction kinetics in combustion. He joined Texas Tech University, Lubbock, in 1996 and is currently an Associate Professor in electrical engineering. His present research interests are high-power microwaves, unipolar surface flashover physics, and explosive-driven pulsed power. He has published more than 100 journal articles and conference proceedings papers.



James C. Dickens (S'89–M'96–SM'04) received the Ph.D. degree in electrical engineering from Texas Tech University, Lubbock, in 1995.

He is an Associate Professor at Texas Tech University. His current research areas include explosively driven pulsed-power generation, investigation of high-efficiency power processing for space applications, electrical space propulsion, high-power vacuum switches, high-power solid-state laser systems, and solid-state opening switches. His past research areas include investigations of electrode erosion in high-power spark-gap switches, high-power microwaves, and the impact of Hall Effect thrusters on communication systems.



Hermann G. Krompholz (SM'84) received the Ph.D. degree in physics from Technical University Darmstadt, Germany, in 1977.

He was a Research Associate at TU Darmstadt from 1977 to 1982, working on nonequilibrium phenomena in high energy density plasmas. From 1982 to 1985, he was with Texas Tech University, Lubbock, with activities in the areas of diffuse discharge opening switches and spark gap erosion. After a brief stay at the Fraunhofer Institute for Laser Engineering and Technology in Aachen, Germany, he rejoined the faculty at Texas Tech University in 1987, where he is now a Professor of electrical and computer engineering/physics. His research interests include several aspects of pulsed power physics and technology, with emphasis on the physics of electrical breakdown in gases and liquids and along surfaces. He has published about 110 journal articles and conference proceedings papers.